Pairing in a two-dimensional Fermi gas with population imbalance

M. J. Wolak,[1] B. Grémaud,[1,2,3] R. T. Scalettar,[4] and G. G. Batrouni[1,5,6]
[1]*Centre for Quantum Technologies, National University of Singapore, 2 Science Drive 3 Singapore 117542*
[2]*Laboratoire Kastler Brossel, UPMC-Paris 6, ENS, CNRS, 4 Place Jussieu, F-75005 Paris, France*
[3]*Department of Physics, National University of Singapore, 2 Science Drive 3, Singapore 117542, Singapore*
[4]*Physics Department, University of California, Davis, California 95616, USA*
[5]*INLN, Université de Nice–Sophia Antipolis, CNRS, 1361 route des Lucioles, 06560 Valbonne, France*
[6]*Institut Universitaire de France*
(Received 21 June 2012; published 23 August 2012)

Pairing in a population-imbalanced Fermi system in a two-dimensional optical lattice is studied using determinant quantum Monte Carlo simulations and mean-field calculations. The approximation-free numerical results show a wide range of stability of the Fulde-Ferrell-Larkin-Ovchinnikov phase. Contrary to claims of fragility with increased dimensionality, we find that this phase is stable across a wide range of values for the polarization, temperature, and interaction strength. Both homogeneous and harmonically trapped systems display pairing with finite center-of-mass momentum, with clear signatures either in momentum space or real space, which could be observed in cold-atomic gases loaded in an optical lattice. We also use the harmonic level basis in the confined system and find that pairs can form between particles occupying different levels, which can be seen as the analog of the finite center-of-mass momentum pairing in the translationally invariant case. Finally, we perform mean-field calculations for the uniform and confined systems and show the results to be in good agreement with quantum Monte Carlo. This leads to a simple picture of the different pairing mechanisms, depending on the filling and confining potential.

DOI: 10.1103/PhysRevA.86.023630 PACS number(s): 03.75.Ss, 71.10.Fd, 74.20.Fg, 02.70.Uu

I. INTRODUCTION

The question of pairing in polarized fermionic systems came to the fore shortly after superconductivity in unpolarized systems was explained by BCS [1] as being due to the formation of Cooper pairs with zero center-of-mass momentum. Fulde and Ferrell [2] and independently Larkin and Ovchinnikov [3] proposed similar but not identical mechanisms whereby the fermions form pairs with nonzero center-of-mass momentum. We will refer to such a phase as the Fulde-Ferrell-Larkin-Ovchinnikov (FFLO) phase. On the other hand, Sarma [4] proposed a mechanism where, in spite of the mismatch in the Fermi momenta due to the spin population imbalance, the pairing occurs with zero center-of-mass momentum. Verifying these predictions experimentally proved difficult in condensed matter systems [5]. However, thanks to rapid experimental progress in the domain of ultracold atoms, it is now possible to study such population-imbalanced systems. Fermionic atoms are made to occupy two hyperfine states, thus emulating a system with "up" and "down" spins. An advantage of these systems is that the population imbalance (the polarization) and the interaction strengths are highly tunable. Such experiments have been performed in three-dimensional [6,7] and one-dimensional [8] systems.

It is by now widely accepted that at $T = 0$ the FFLO phase is robust over a wide range of parameters in one-dimensional systems with imbalanced fermion populations. This was shown in various numerical studies using, for example, quantum Monte Carlo (QMC) [9,10] and density-matrix renormalization group (DMRG) [11–15]. In addition, it has been shown to be stable in quasi-one-dimensional situations, i.e., in the case of an elongated trap [16,17]. In a previous work, we also showed that the FFLO phase is stable over a wide range of parameters in the temperature-polarization (TP) phase diagram [18]. This exotic pairing occurs both in homogeneous and confined systems, and has been shown to survive up to relatively high temperatures ($T/T_F \approx 0.1$) which are achievable in current experiments.

The question of the stability of this phase in higher dimensions remains a subject of debate. It is believed that "nesting" of the Fermi surfaces stabilizes FFLO pairing. For example, in one dimension one wave vector connects all points on the Fermi surfaces of each species, which would enable all particles from the Fermi surfaces to participate in the formation of pairs with finite momentum. The effect of "nesting" is considerably weaker in higher dimensions. In a two-dimensional lattice system, the shape of a Fermi surface depends on the filling. At half-filling, the Fermi surface becomes a square and touches the edge of the first Brillouin zone (van Hove singularity). Around this filling, matching of the Fermi surfaces becomes more efficient, in other words, the "nesting" is enhanced as compared to the situation when both Fermi surfaces are circular (low filling). This reasoning leads us to expect that FFLO pairing should be more prevalent around half-filling than at lower fillings. This lattice-enhanced stability of FFLO was studied using mean-field (MF) methods in Refs. [19] and [20]. In the latter, the authors point also at Hartree corrections and domain-wall formation as additional reasons for enhancement.

Numerous theoretical studies of the system in higher dimensions do not offer a clear conclusion on the stability of the FFLO mechanism. In a variational MF study of a three-dimensional system in the continuum with and without

a trapping potential, it is observed that FFLO is a fragile state which can be realized only in a tiny sliver of the interaction-polarization phase diagram [21,22]. Furthermore, this study showed that in a trap, FFLO can exist only in a thin shell of the atomic cloud. Another study of a three-dimensional Fermi gas at unitarity [23] shows that this phase is competitive over a large region in the phase diagram. However, the trap would need to be adjusted to allow FFLO to occupy a large enough spatial region to be observed. On the other hand, in a Bogoliubov–de Gennes study [24] of a trapped system, the calculated phase diagram indicates that the ground state of the system is always FFLO for any imbalance up to some critical value.

The unsettled status of this phase in higher dimensionality may be clarified with exact numerical simulations. However, simulations of the Hubbard model in three dimensions are not feasible for large systems at low enough temperatures due to the severity of the "fermion sign problem." On the other hand, exact QMC simulations in two dimensions are feasible, but so far none have demonstrated the existence of the FFLO order in fermionic systems. In addition, two-dimensional systems are intermediate between one dimension where MF is almost certain to fail and three dimensions where MF is more reliable. Consequently, there has been a concerted, yet inconclusive, effort to understand FFLO physics theoretically in two-dimensional systems. Homogeneous and trapped two-dimensional polarized Fermi gases have been studied with MF calculations which exclude the possibility of FFLO pairing (e.g., [25] and [26]). An interaction-polarization phase diagram is shown in Ref. [27] where FFLO pairing is seen to occupy a wide region. Koponen *et al.* [19] obtain MF phase diagrams in the polarization versus filling plane for one-, two-, and three-dimensional systems. In the two-dimensional system, there is a very strong feature around the van Hove singularity of the majority component and the FFLO phase is present over a wide range of parameters around this value. They also show temperature-polarization phase diagrams of one dimensional system which were shown not to agree with exact QMC results [18]. The temperature-polarization phase diagram in three dimensions is shown as well but not the two-dimensional case. Studies of quasi-two-dimensional systems have been done using MF and they predict a first-order transition to FFLO at finite temperature [28]. Another mean-field study of two-dimensional two-orbital Hubbard model with p orbitals and highly unidirectional hopping shows enhancement of the FFLO region in the phase diagram due to the one-dimensional character of the Fermi surface [29]. A DMRG study of population imbalanced Fermi gas on two-leg ladders has found FFLO pair correlations [30].

In this paper, we present a determinant QMC (DQMC) [31] study of the two-dimensional Hubbard model with imbalanced populations of up and down spins. In Sec. II, we present the model and discuss our results for the uniform system in Sec. III. Our main result here is the demonstration of the robustness of the FFLO phase and the determination of the phase diagram in the temperature-polarization plane at low filling. We also compare the behavior of the system at low and half-fillings. In Sec. IV, we examine the system in a harmonic trap. Our conclusions are in Sec. V.

II. MODEL AND METHODS

The system of interest is governed by the two-dimensional fermionic Hubbard Hamiltonian

$$\begin{aligned} H = &-t \sum_{\langle i,j\rangle \sigma} (c^\dagger_{i\sigma} c_{j\sigma} + c^\dagger_{j\sigma} c_{i\sigma}) - \sum_i (\mu_1 \hat{n}_{i1} + \mu_2 \hat{n}_{i2}) \\ &+ U \sum_i \left(\hat{n}_{i1} - \frac{1}{2}\right)\left(\hat{n}_{i2} - \frac{1}{2}\right) \\ &+ V_T \sum_j (j - j_c)^2 (\hat{n}_{j1} + \hat{n}_{j2}), \end{aligned} \tag{1}$$

where $c^\dagger_{i\sigma}$ ($c_{i\sigma}$) create (annihilate) a fermion of spin $\sigma = 1, 2$ on lattice site i (the lattice spacing is equal to unity, setting both spatial and momentum scales) and $\hat{n}_{i\sigma} = c^\dagger_{i\sigma} c_{i\sigma}$ is the corresponding number operator. The near-neighbor $\langle i, j\rangle$ hopping parameter is t, which we take equal to unity to set the energy scale. We consider only onsite interaction with an attractive coupling constant $U < 0$. The number of particles in each population is governed by its chemical potential (μ_σ). The harmonic trap is introduced via the V_T term in the Hamiltonian where j_c is the position of the center of the trap (also middle of the lattice). All simulations are performed with periodic boundary conditions. In the confined case, we ensured that the density vanishes at the edge of the lattice.

The main quantities of interest in this study are the single-particle Green's functions G_σ and the pair Green's function G_{pair}:

$$G_\sigma(l) = \langle c^\dagger_{i+l\sigma} c_{i\sigma} \rangle, \tag{2}$$

$$G_{\text{pair}}(l) = \langle \Delta^\dagger_{i+l} \Delta_i \rangle, \tag{3}$$

$$\Delta_i = c_{i2}\, c_{i1}, \tag{4}$$

where Δ_i creates a pair on site i. The Fourier transform of G_σ gives the momentum distribution of the spins-σ species while the transform of G_{pair} yields the pair momentum distribution. In the trapped case, the density profiles of the two species are also studied.

We studied this system numerically using the DQMC [31] algorithm. In this approach, the Hubbard-Stratonovich (HS) transformation is employed to decouple the quartic interaction term into two quadratic terms coupling the number operator of each species $n_\sigma(i)$ to the HS field, which effectively acts as a site-dependent and imaginary-time-dependent chemical potential. The fermion operators can now be traced out leading to a partition function in the form of a product of two determinants, one for each spin, summed over all configurations of the HS field. For $U < 0$ and equal populations $\mu_1 = \mu_2$, the determinants are identical: their product is always positive. But, in the imbalanced case $\mu_1 \neq \mu_2$, the two determinants are no longer equal and their product can, and does, become negative leading to the known "fermion sign problem." This is the main obstacle to the simulation of this system. We found that at low total filling the sign problem is manageable even at large polarizations and low temperatures. This was not the case closer to half-filling. Typical simulations of the harmonically confined system at low temperature took about two weeks on a 3-GHz processor.

In the presence of the trapping potential, we have also studied the system using a mean-field approach. Starting from the full Fermi-Hubbard Hamiltonian (1), one can derive the mean-field Hamiltonian:

$$H_{\mathrm{MF}} = \psi^{\dagger} M \psi + \frac{1}{U} \sum_i \Delta_i^* \Delta_i - \sum_i \mu_{i\,2},$$
$$M = \begin{pmatrix} h_{ij\,1} & -\Delta_i \\ -\Delta_i^* & -h_{ji\,2} \end{pmatrix}, \tag{5}$$

where $\Delta_i^* = U\langle c_{i\,1}^{\dagger} c_{i\,2}^{\dagger}\rangle$ are onsite pairing amplitudes; $\Psi^{\dagger} = (\ldots, c_{i\,1}^{\dagger}, \ldots, c_{i\,2}, \ldots)$ is the Nambu spinor. The matrix h depicts the one-particle Hamiltonian, namely, hopping terms between nearest neighbors $h_{ij\sigma} = -t \quad (i \neq j)$ and chemical potential terms $h_{jj\sigma} = -\mu_{j\sigma} = -\mu_{\sigma} + V_T(j - j_c)^2 \hat{n}_{j\,\sigma}$. To account properly for spatial inhomogeneities, the BCS order parameter at each site, Δ_i, is an independent variable [32–34], whose value is determined, for a given temperature, by a global minimization of the free energy $F = -\frac{1}{\beta} \ln(\mathcal{Z})$ associated with the mean-field Hamiltonian:

$$F = -\frac{1}{\beta} \sum_k \ln(1 + e^{-\beta\lambda_k}) + \frac{1}{U} \sum_i \Delta_i^* \Delta_i - \sum_i \mu_{i\,2}, \tag{6}$$

where the λ_k are the $2N$ eigenvalues of the Nambu matrix M; N is the number of sites. β is the inverse (dimensionless) temperature $1/T$. The minimization of the free energy is performed using a mixed quasi-Newton and conjugate gradient method; additional checks were performed to ensure that the global minimum has been reached.

III. HOMOGENEOUS SYSTEM

To set the stage, we start with the homogeneous two-dimensional Hubbard model with balanced populations at total density $\rho = \rho_1 + \rho_2 = 0.3$. With balanced populations, the pairs form with zero center-of-mass momentum and a sharp peak in the pair momentum distribution is expected at $\vec{k} = 0$. Figure 1 shows the momentum distributions for a system with $U = -3.5$, $\rho_1 + \rho_2 = 0.3$, and $\beta = 30$ in a 16×16 optical lattice. The single-particle momentum distribution, identical for the two spins, is shown in Fig. 1(a), while Fig. 1(b) shows the pair momentum distribution. As expected for weak to moderate values of $|U|$, the single-particle distribution has the usual Fermi form and the pair momentum distribution exhibits a very sharp peak at $\vec{k} = 0$, indicating pairing with zero center-of-mass momentum.

We now examine the polarized system. To this end, the chemical potentials μ_1 and μ_2 are made unequal so that $\rho_1 \neq \rho_2$ but $\rho = \rho_1 + \rho_2$ remains constant. This requires tuning the chemical potentials appropriately. The polarization P is defined by

$$P = \frac{N_1 - N_2}{N_1 + N_2}, \tag{7}$$

where N_1 and N_2 are the total populations of the two species.

Figure 2 shows the momentum distributions for a system with $U = -3.5$, $P = 0.6$, $\rho = 0.3$, and $\beta = 10$ in an optical lattice of size 16×16 for Figs. 2(a)–2(c) and 10×30 for Fig. 2(d). Figures 2(a) and 2(b) show the minority and majority single-particle momentum distributions $n_1(k_x,k_y)$ and

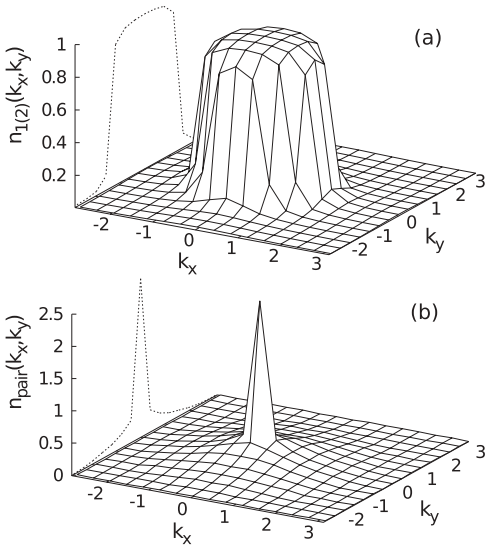

FIG. 1. (a) Single-particle momentum distribution $n_1(k_x,k_y)$ [the same as $n_2(k_x,k_y)$]. (b) Pair momentum distribution $n_{\mathrm{pair}}(k_x,k_y)$ exhibiting a sharp peak at zero momentum. The total density is $\rho_1 + \rho_2 = 0.3$ ($\rho_1 = \rho_2$), $\beta = 30$, $U = -3.5$, and the system size is 16×16.

$n_2(k_x,k_y)$, respectively. They exhibit usual Fermi-type distributions. However, the pair momentum distribution $n_{\mathrm{pair}}(k_x,k_y)$ is strikingly different from the balanced case: It has a volcanolike shape with the maximum of the distribution at the rim of the crater of radius $|\vec{k}| = |\vec{k}_{F2} - \vec{k}_{F1}|$. $\vec{k}_{F1}$ and $\vec{k}_{F2}$ are the minority and majority Fermi momenta, respectively.

In two dimensions, the Fermi surface geometry changes with the filling. The behavior exhibited in Fig. 2 is for low filling where the Fermi distributions of both species have cylindrical shape and the pairs are formed with equal probability in all radial directions. In this density regime, the signature for the FFLO phase is the presence of a circular ridge in the pair momentum distribution as seen in Fig. 2(c). Studying the system in the low density regime is interesting because it also approximates the continuum conditions.

To study possible finite-size effects, we performed our simulations for systems of various sizes. In particular, Fig. 2(d) shows the pair momentum distribution for the same parameters as Figs. 2(a)–2(c), but with a system of size 10×30. It is seen that the peak in the pair momentum distribution is at the same values of $|\vec{k}| = |\vec{k}_{F1} - \vec{k}_{F2}|$ as the 16×16 system.

We now examine the effect of temperature on the FFLO phase. In particular, we map out the phase diagram in the temperature-polarization plane. Thermal effects are very important in experiments due to the difficulty in cooling fermionic atoms. The inset in Fig. 3 shows two-dimensional cuts in the three-dimensional pair momentum distribution for a 16×16 system with $U = -3.5$, $\rho = 0.3$, and $P = 0.55$. We see that as the temperature is increased (β decreased), the FFLO peak at nonzero momentum decreases and, in fact, shifts towards zero momentum. Our criterion for the appearance of the FFLO phase is when the peak of the pair momentum distribution is no longer at zero momentum. The question is then what replaces the FFLO phase: Have the pairs been broken by thermal fluctuations or has the system been homogenized,

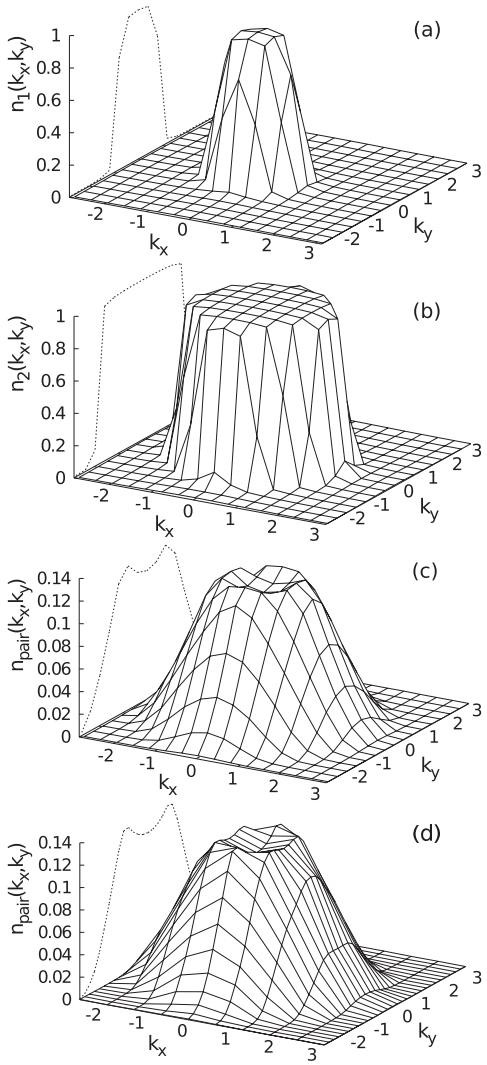

FIG. 2. Momentum distributions of (a) minority and (b) majority populations. (c) Shows the pair momentum distribution. The parameters are $\rho = \rho_1 + \rho_2 = 0.3, P = 0.6, \beta = 10, U = -3.5$ in an optical lattice of size 16×16. (d) The pair momentum distribution for the same system but for a lattice of size 10×30.

resulting in a uniform mixture of pairs and excess unpaired particles of the majority population? The double occupancy $D = \langle n_1(\vec{r}) n_2(\vec{r}) \rangle$ offers a measure of how tightly bound the pairs are: In the absence of pairing, $D = \rho_1 \rho_2$ while when the pairing is complete, $D = \rho_1$ where ρ_1 is the minority population. These limits suggest the use of a normalized form $(D - \rho_1\rho_2)/(\rho_1 - \rho_1\rho_2)$, which is now bounded by 0 and 1. Note that $\rho_1 = N_1/L^2$ while $\langle n_1(\vec{r}) \rangle$ is the average number of type-1 particles at $\vec{r}$. In the absence of pairing, the two quantities coincide. We see in Fig. 3 that for $\beta > 3$ the normalized double occupancy is essentially constant, signaling the continued presence of pairs. This means that when the FFLO peak first disappears at $4 < \beta < 3$, the pairs are still formed. We conclude therefore that the system leaves the FFLO phase to enter a polarized paired phase (PPP) phase.

When the thermal energy $T = 1/\beta$ is of the order of the pair binding energy $|U|$, the pairs are expected to break. We see in Fig. 3 that the double occupancy decreases precipitously

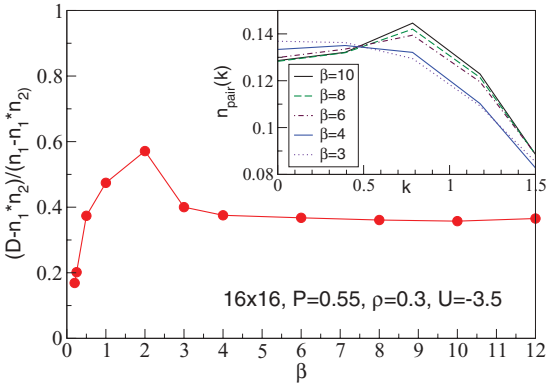

FIG. 3. (Color online) The normalized double occupancy as a function of inverse temperature β for $\rho = 0.3$, $P = 0.55$, and $U = -3.5$. The lattice size is 16×16. Inset: Behavior of the pair momentum distribution as the temperature is increased (β is decreased).

only for $\beta < 1$, which is consistent with the value of $1/|U| = 1/3.5$ in our simulation. Similar behavior was found for the one-dimensional system [18].

Note in Fig. 3 that the double occupancy increases just before it drops, signaling the breaking of the pairs. This increase can be understood physically as follows. As the temperature is increased, the Fermi distribution near the Fermi momentum gets rounded, but for $|\vec{k}| < |\vec{k}_F|$ the distribution remains saturated. This means that pairing can happen only near the Fermi surface, while inside the Fermi sea the particles are still blocked by the Pauli exclusion principle. Eventually, as T continues to increase, the occupation of momentum states inside the Fermi sea drops, rather suddenly as shown by our simulations, which makes available for pairing a larger number of particles causing the double occupancy to rise.

The phase diagram is mapped by fixing the polarization P and increasing T until the peak in the pair momentum distribution shifts to zero momentum (inset Fig. 3). The phase diagram for $\rho = \rho_1 + \rho_2 = 0.3$ (circles) and $\rho = 1$ (squares) is shown in Fig. 4. The solid circles show the boundary of the FFLO phase; the open circles indicate the largest P at which we were able to study the system. Up to these high polarizations, the system remained in the FFLO phase. The

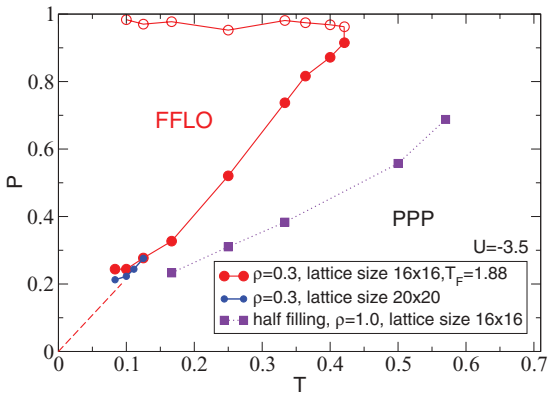

FIG. 4. (Color online) Finite-temperature phase diagram of the system at $\rho = 0.3$.

FFLO phase boundary at low P appears to extrapolate to $P \neq 0$ as $T \to 0$ for the 16×16 system. However, this is an effect of the coarseness of the lattice grid. As P decreases, the peak in the pair momentum distribution falls between 0 and $2\pi/L$ and gives the impression of peaking at zero momentum. The blue circles show the phase boundary for a 20×20 system; we see that effect is corrected for a while, but then even larger systems are needed. This is not possible because as T decreases, the sign problem becomes too severe. We believe that as soon as the system is polarized it goes into the FFLO phase if T is low enough. The long dashed line connecting this FFLO boundary to the origin schematizes this. Outside the FFLO phase, the system is in the PPP since the pairs are still formed and break only at higher T than shown in the figure. The squares in Fig. 4 show the phase boundary at these temperatures for the case of $\rho = 1$ (discussed in the following).

It is important to emphasize here that, in our discussion, the FFLO state is characterized by the behavior of the pair momentum distribution: If the peak is at nonzero momentum, the system is in the FFLO phase. The question naturally arises as to whether the FFLO pairs have phase coherence and are, consequently, superfluid. In the balanced case, the phase diagram in the temperature versus filling plane was determined for $U = -4$ in Ref. [35]. By studying the pairing susceptibility as a function of T as in Ref. [35], we find that in the balanced case of our system with $U = -3.5$, the critical temperature is $T_c \approx 0.1$, in good agreement with the $U = -4$ results [35]. However, studying the same pairing susceptibility in the polarized case showed no sign of s-wave superfluidity in the temperature range attainable by QMC. Our numerical results support approximate analytic results which indicate that polarization may suppress superfluidity in the FFLO phase [36]. It is, therefore, currently not clear if when T is reduced even further, the FFLO phase will become superfluid. We note, however, that the current focus of most experimental measures of FFLO is the same nonzero momentum peak on which our simulations concentrate.

The phase diagram (Fig. 4) resembles the one found in one dimension [18] and shows that FFLO is very robust. The Fermi temperature is calculated as usual by considering a balanced ideal system and gives for $\rho = 0.3$ a value $T_F = 1.88t$. The FFLO phase at high P survives up to $T = 0.2T_F$, while in one dimension [18] at $\rho = 0.25$, FFLO survives up to $T = 0.8T_F$ at high P. So, while FFLO is still robust in two dimensions, it is more easily destroyed by finite T. This is important to keep in mind in experiments.

In a two-dimensional lattice, the Fermi surface geometry evolves with the filling from closed, rotationally symmetric surfaces for low filling to a square at half-filling to open surfaces for higher filling. Consequently, pairing at finite momentum occurs with different symmetries depending on the filling. The pairs form with equal probability in all radial directions in the case of low filling while they form in preferred directions when the Fermi surfaces are anisotropic.

As discussed in the Introduction, there are claims that around the van Hove singularity the FFLO pairing could be enhanced due to increased nesting. Indeed, we observe that FFLO is stable over a wider range of temperatures and polarizations for $\rho = 1$. The squares in Fig. 4 show the FFLO-PPP boundary in the half-filled case. It is seen that

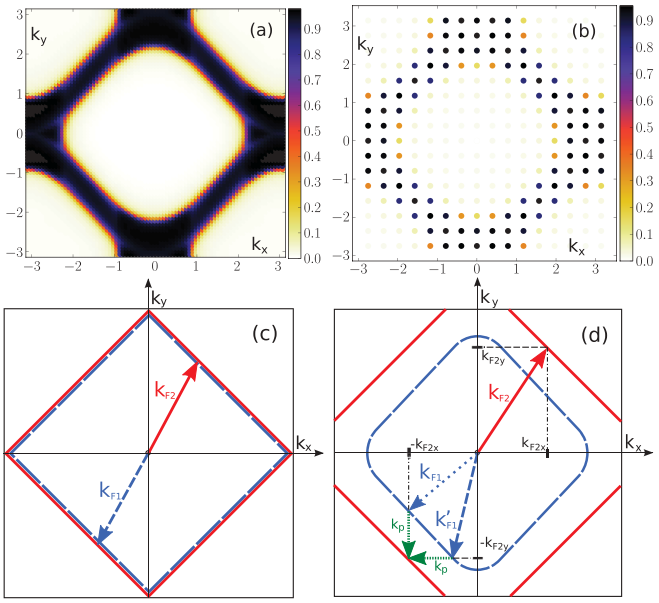

FIG. 5. (Color online) Top row: difference in the momentum distributions of majority and minority, showing parallel Fermi surfaces from the mean-field method (a) and from QMC (b). Bottom row: pairing schematic for balanced (c) and imbalanced (d). In the situation when the populations of fermionic species are imbalanced (diagram on the right), a particle from the majority species forms a pair with a particle from the minority, the Fermi momentum of which either matches the k_x or k_y coordinate of the majority particle Fermi vector. The pair formed has a finite momentum equal to the distance of the two Fermi surfaces either along k_x or k_y.

the FFLO phase persists to higher T than the low-density case. However, when compared to $T_F = 6.28t$, FFLO is destroyed for $T \approx 0.08T_F$ as compared with $T \approx 0.2T_F$ for the half-filled case in one dimension.

When the populations are imbalanced around half-filling of the lattice, one can readily see the effect of the interaction on the Fermi surfaces in Fig. 5, depicting the difference between the Fermi distributions of the species calculated using both mean-field and QMC methods: they almost look like nested squares parallel to each other in most of the momentum states, whereas the noninteracting ones would look more rounded and not as parallel. Similar Fermi surface geometry in the context of LO states in three dimensions (3D) have been shown in Ref. [20].

The reason why the system exhibits such Fermi surfaces can be understood as follows. If we look at the region of $k_x > 0$, we can parametrize the linear part of the majority Fermi line as $k^+_{f,2}(k_x) = -k_x + \alpha_2$ for positive values and $k^-_{f,2}(k_x) = k_x - \alpha_2$ for negative values and doing the same for the minority we have $k^+_{f,1}(k_x) = -k_x + \alpha_1$ and $k^-_{f,1}(k_x) = k_x - \alpha_1$ (see Fig. 5). Pairing happens here for a given k_x between the upper part of the majority branch and the lower part of the minority branch [$k^+_{f2}(k_x)$ pairs with $k^-_{f1}(-k_x)$]. The momentum of the pair along y is the sum of these momenta and is equal to $q_y = k^+_{f2}(k_x) + k^-_{f1}(-k_x) = \alpha_2 - \alpha_1$. Therefore, thanks to the parallel Fermi lines, the pairing momentum is independent of k_x, leading to a strong enhancement of the pairing efficiency. The same construction can be done in the

k_x direction, matching the y coordinate of the momentum vectors and the pairs will be moving along x with $\pm q_x$. In other words, for each k_x, we have, along k_y the usual imbalanced one-dimensional (1D) situation, i.e., two rectangular Fermi distributions, with different Fermi momenta. Again, the crucial point is both the majority and minority effective 1D Fermi momentum values change the same way with k_x: the two Fermi surfaces remain always at the same distance from each other. This pairing mechanism is illustrated in Fig. 5(d). The excess fermions correspond to the part of the majority Fermi surface which can not be paired this way, i.e., the four regions around $(k_x = 0, ky = \pm\pi)$ and $(k_x = \pm\pi, ky = 0)$. Note that in the balanced case, this corresponds to the usual BCS pairing on a lattice: a particle of one species from the Fermi surface can form a pair with a particle from the other species with the Fermi vector of equal length but opposite direction [as shown in Fig. 5(c)]. The resulting pair has, as expected, a zero center-of-mass momentum. The pairing along k_x and k_y might not seem the most intuitive scenario since one can imagine the pairs forming with momentum along the diagonal with smaller $|\vec{k}_p|$. Since this pairing was not observed in any of our simulations, this probably means that, in a mean-field approach, it only corresponds to a local minimum of the free energy. However, since the shape of Fermi surfaces is affected by the nature of the pairing, one can not directly compare both situations from the present results and a more detailed study is needed, which is beyond the scope of this paper. On the contrary, the mean-field simulations show sharp peaks either along k_x or k_y depending on the realization (see Fig. 6), and in the quantum Monte Carlo simulations since we average over all realizations, we see that the pair momentum distribution exhibits four peaks: two along k_x and two along k_y (see Fig. 7). It is important to notice a very good agreement between the results obtained by MF and QMC methods. Finally, we have also observed, as expected, that the value of the position of the peaks, i.e., the center of mass of the pairs, increases with large population imbalance.

IV. HARMONICALLY CONFINED SYSTEM

One is used to describing free fermions on a lattice using intuition built on the free-electron model. Each particle occupies a state with particular momentum $\vec{k}$, and at $T = 0$ the filled state with the highest $\vec{k}$ is called the Fermi level. BCS pairing mechanism is understood as pairing between fermions from the Fermi surface with opposite spins and opposite momenta. In this description, the FFLO pairing model predicts forming a pair of fermions from different spin species with a finite momentum, where the momentum of the pair is the difference of the Fermi momenta of each involved fermion. When we turn to study a harmonically confined system at low filling, for which only few harmonic levels are actually filled, the translationally invariant momentum space description is no longer the obvious one. An ideal gas confined in a harmonic trap is known to be fully characterized by the basis formed by harmonic-oscillator wave functions. In addition, for low fillings of the lattice, only the bottom of the band structure will be filled. Then, the kinetic part of the Hamiltonian is well described by the free-particle one with an effective mass m^* given by $m^* = 1/2a^2t$, where a is the lattice spacing and t

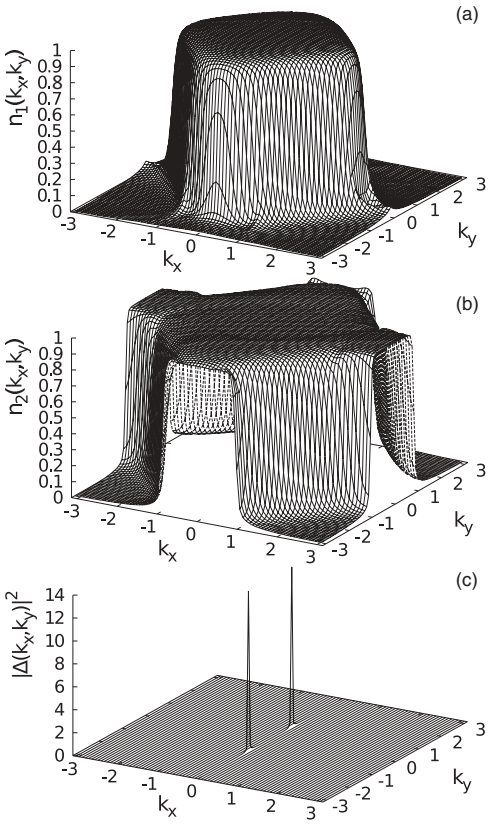

FIG. 6. Momentum distributions of (a) minority, (b) majority, and (c) order parameter in k space calculated using the mean-field method. $\rho = \rho_1 + \rho_2 = 1$. Here, $P = 0.32$, $\beta = 25$, $U = -3.5t$, and the lattice size is 79×79. The pairing peaks are symmetric along k_x or k_y depending on the realization.

the tunneling amplitude. In the present case, setting the units $t = 1$ and $a = 1$, the effective mass is therefore $m^* = 1/2$.

In this section of the paper, we explore the description of the interacting system in the harmonic basis. This transformation is the analog of the Fourier transformation used to go from real space to momentum space in the case of the free system. We will show that both BCS and FFLO models can be translated into the harmonic level basis as pairing of particles between harmonic levels and look into the limitations of this description. Since we are studying a two-dimensional system, we use the eigenstates of the two-dimensional harmonic oscillator (see, for example, [37]). Due to rotational symmetry, the nth harmonic level is $n + 1$ times degenerate. We will use the labeling of the states as follows: n is the principal quantum number and $m = -n, -n + 2, \ldots, n$ is the orbital angular momentum quantum number. For simplicity, we will sometimes use κ to label the set of quantum numbers, $\kappa = (n,m)$. Taking the normalized harmonic-oscillator wave function for a particular level to be $\Phi_{n,m}(i)$ (where i is the lattice site), we define a creation operator of a particle in a level as

$$\Psi^\dagger_{n,m} = \frac{1}{\sqrt{N}} \sum_i \Phi^*_{n,m}(i) c^\dagger_i, \tag{8}$$

which, in the continuum limit, leads to properly anticommutating fermionic operators.

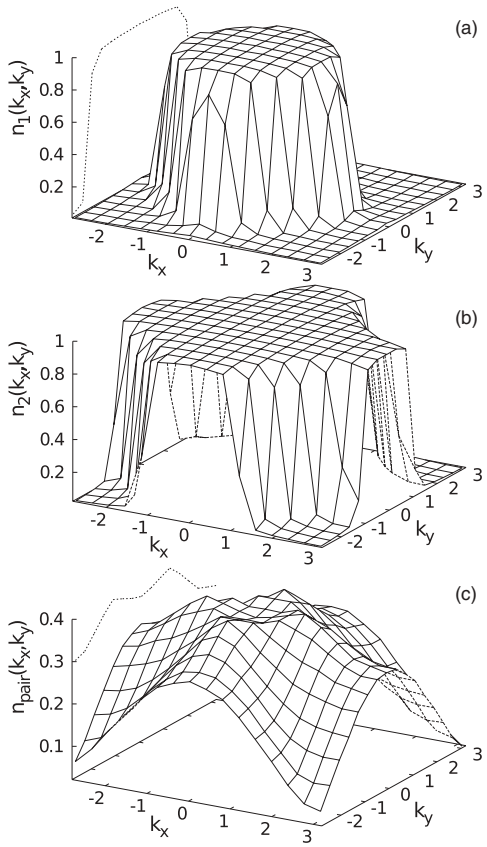

FIG. 7. Momentum distributions of (a) minority, (b) majority, and (c) pairs at $\rho = \rho_1 + \rho_2 = 1$, obtained from QMC. Here, $P = 0.38$, $\beta = 10$, $U = -3.5$, and the lattice size is 16×16. The pair momentum distribution depicts four peaks along the k_x and k_y axes.

We calculate the single-particle Green's function between levels for each species as follows:

$$G_\sigma(\kappa,\kappa') = \langle \Psi^\dagger_{\kappa,\sigma} \Psi_{\kappa',\sigma} \rangle. \tag{9}$$

As pairing is our main interest of investigations, we also define a pair Green's function using the creation and annihilation operators of a pair of fermions. Similarly to the homogeneous case where the pairs are formed between particles having different momenta, the pairs here can have constituents occupying different harmonic levels:

$$G_{\text{pair}}(\kappa,\kappa') = \langle \Psi^\dagger_{\kappa',1} \Psi^\dagger_{\kappa,2} \Psi_{\kappa,2} \Psi_{\kappa',1} \rangle. \tag{10}$$

Therefore, the usual BCS pairing with opposite momenta $\vec{k} \leftrightarrow -\vec{k}$ corresponds to a pairing $(n,m) \leftrightarrow (n,-m)$, i.e., to fermions having the same principal quantum number and opposite magnetic number. The FFLO pairing $\vec{k} \leftrightarrow -\vec{k}'$, for which the norm of the momenta is different, corresponds to a pairing $(n,m) \leftrightarrow (n',-m')$ between fermions having different principal quantum number, i.e., between fermions from different energy levels.

In this section, we present results for these correlation functions obtained using both QMC and MF methods of balanced and polarized systems with low filling of the lattice. All QMC results were done on a 20×20 lattice at the inverse temperature $\beta = 10$ with interaction strength $U = -3.5$ and the trap potential $V_t = 0.065$, which translates to an effective

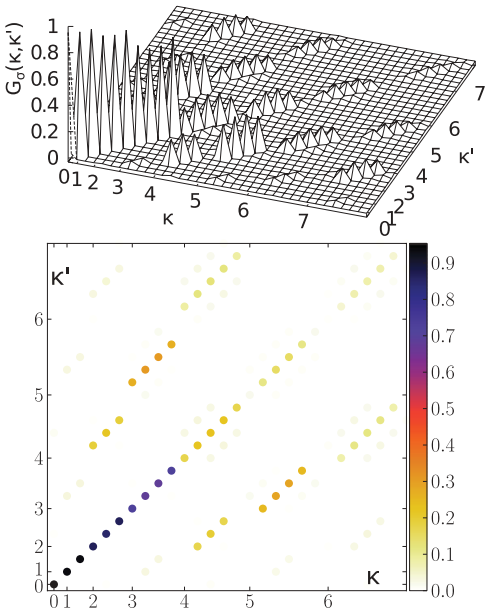

FIG. 8. (Color online) Single-particle Green's function in the harmonic level basis using QMC in the balanced case. The total number of particles is 22.3, i.e., ≈11 particles per spin. As one can see, the single-particle Green's function value on the diagonal sharply drops just before the fifth level ($n = 4$) corresponding to 10 harmonic states, roughly the number of particles per spin. The off-diagonal elements are small compared to the diagonal ones, emphasizing the accuracy of the harmonic description of the system. States are labeled with $\kappa = (n,m)$ and only the principal quantum number n is displayed on the x and y axes.

harmonic frequency $\omega = 0.5$. The simulations done using the mean-field method were performed on a bigger lattice of 41×41 sites, at the inverse temperature of $\beta = 25$ and taking the interaction strength to be $U = -3.0$ In the figures, only the n values are explicitly written, but correlations are calculated between all different n and m values. The m levels are arranged from $m = -n$ to n from left to right (or bottom to top). In the balanced case shown in Fig. 8, the single-particle Green's function is mainly diagonal, which indicates that in this regime the harmonic level basis offers a good description of the system. The diagonal part is the occupation of levels and where it drops to zero one can define the Fermi level. We compare these results to those obtained using the mean-field method. Both single particle as well as pair Green's function shown in Fig. 10 agree qualitatively to the QMC results. The small of-diagonal values in QMC, which are not present in the MF results, stem from the exact treatment of the interactions in QMC, not taken into account in the MF calculations. In the regime of much higher fillings of the lattice (for example around half-filling), the effective mass approach is no longer valid and the MF results show that the harmonic basis is no longer a relevant one. We do not have any QMC results in that regime due to the sign problem.

In the balanced population case, both Figs. 9 (QMC) and 10 (MF) emphasize that the pairing is maximum around the Fermi level and happen between particles from levels with the same n and for opposite m and m' values such that the total orbital angular momentum of the pair is 0. This situation

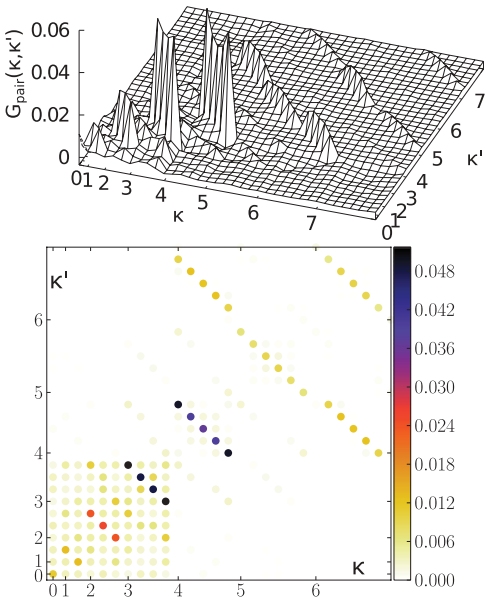

FIG. 9. (Color online) Pair Green's function in the harmonic level basis using QMC. The total number of particles is 22.3 and the populations are balanced. One can clearly see that the pairing is maximum at the Fermi level $n = 4$–5, with opposite magnetic quantum numbers m. Off-diagonal pairing, e.g., between $\kappa = (6,m)$ and $\kappa' = (4,m')$, is almost negligible. By diagonal pairing, we mean pairing between levels with equal principal quantum numbers.

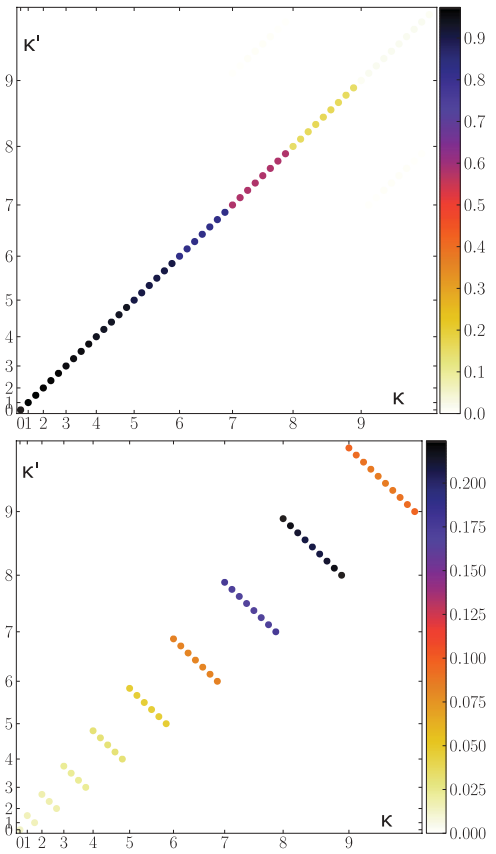

FIG. 10. (Color online) Single particle and pair Green's function in the harmonic level basis using MF. Total number of particles is 80.4 and the populations are balanced. As in Fig. 8, the single-particle Green's function is diagonal, with a value equal to 1 up to the Fermi level ($n \approx 8$) dropping to 0 after. The pair Green's function emphasizes the diagonal pairing $(n,m) \leftrightarrow (n,-m)$.

is similar to the free-particle case, where the pairing occurs mostly between the $+\vec{k}_F$ and $-\vec{k}_F$ states.

At low imbalance, one observes that the pairing mostly occurs between the same levels, for instance in Fig. 11, where one observes diagonal pairing for $n = 3$ and 4. However, one observes an off-diagonal feature appearing that corresponds to pairing between the levels $n = 3$ and 4. When the system is imbalanced even more, the off-diagonal feature becomes the main pairing amplitude. For instance, as shown in Fig. 12, corresponding to a polarization $P = 0.22$, the diagonal pairing has almost completely disappeared and the pairing mostly occurs between the levels $n = 3$ and 4. Since it corresponds to a pairing between an odd and even level, it is impossible to match the m values and get the pairing with total angular momentum zero. We observed that the strongest pairing happens, for example, between $\kappa = (4,-4)$ and $\kappa' = (3,3)$ and analogously between $\kappa = (4,4)$ and $\kappa' = (3,-3)$. There is, in addition, a small contribution from the levels $\kappa = (4,-2)$ and $\kappa' = (3,1)$ and $\kappa = (4,2)$ and $\kappa' = (3,-1)$. In both cases, the sum of the orbital angular momentum is nonzero. Imbalancing the system even more, we arrive at the situation where the difference between the Fermi levels of each species is $n_{F2} - n_{F1} = 2$. As illustrated in Fig. 13 for $P = 0.37$, the pairing occurs between the levels $n = 5$ and 3 and also $n = 4$ and 2, which means that the system can now achieve pairing with zero total orbital angular momentum. Still, there is small contribution of pairing between $\kappa = (5,-5)$ and $\kappa' = (3,3)$ and $\kappa = (5,5)$ and $\kappa' = (3,-3)$, for which $\Delta m = \pm 2$. For a comparison, we show the results from the mean-field simulations, depicting a similar behavior. In the realization shown in Fig. 14, the Fermi levels of each species are $n = 7$ and 9 and we can see the pairing occurs between those levels as well as between the two levels below $n = 6$ and 8. The largest m values are almost unpaired, for they would have led to nonzero total angular momentum. We conclude that in the low-filling regime and at intermediate interaction strength, we can understand the FFLO pairing mechanism in a trapped system as pairing between fermions from different harmonic levels. We observe that the pairs are formed in such a way so that the total orbital angular momentum of all pairs is always zero, and the orbital angular momentum is minimized for each pair. Finally, similarly to the untrapped case where the pairs are produced with a finite center-of-mass momentum (vanishing for the balanced case), the FFLO state in the harmonic trap corresponds, in a classical picture, to pairs whose center of mass is oscillating around the minimum of the trap with an amplitude increasing with population imbalance.

Momentum distributions and density profiles at low filling of the lattice. Fermion systems with imbalanced populations have been realized experimentally in one-dimensional and elongated three-dimensional harmonic traps. The density profiles of the populations were found to be qualitatively different in the two cases. In three dimensions, one observes the formation of concentric shells where, for very low polarization, the core is fully paired, i.e., zero local magnetization, and

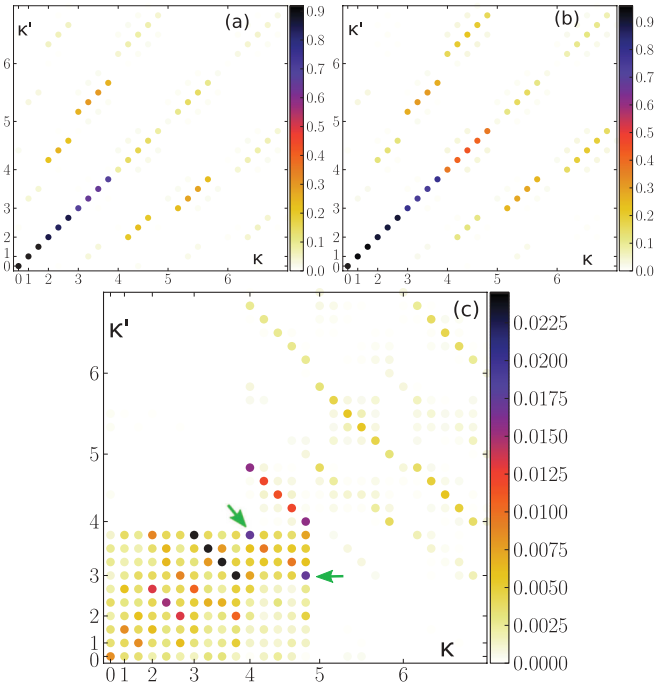

FIG. 11. (Color online) Single particle (a) and (b) and pair Green's functions (c) in the harmonic level basis (QMC results) for a low polarization situation ($P = 0.11$). The total number of particles is 25.5. Even though the Fermi levels between the two species no longer match, the pairing is still diagonal for $n = 3$ and 4 levels. However, one observes an off-diagonal feature appearing that corresponds to pairing between the levels $\kappa = (4,-4)$ and $\kappa' = (3,3)$ and, respectively, $\kappa = (4,4)$ and $\kappa' = (3,-3)$ as indicated by arrows.

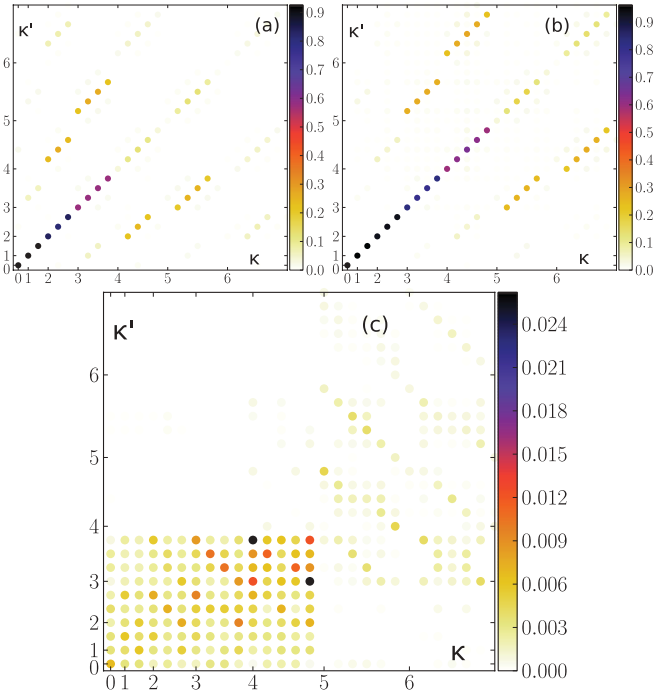

FIG. 12. (Color online) Single particle (a) and (b) and pair (c) Green's functions in the harmonic level basis (QMC results) for a medium polarization ($P = 0.22$). The total number of particles is 26.9. The diagonal pairing has almost completely disappeared and the pairing mostly occurs between the levels $n = 3$ and 4. More precisely, the strongest pairing occurs between $\kappa = (4,-4)$ and $\kappa' = (3,3)$ and analogously between $\kappa = (4,4)$ and $\kappa' = (3,-3)$. There is, in addition, a small contribution from the levels $\kappa = (4,-2)$ and $\kappa' = (3,1)$ and $\kappa = (4,2)$ and $\kappa' = (3,-1)$. Note that each pairing corresponds to a nonvanishing total angular momentum for the pair.

the wings are partially polarized [6,7]. On the other hand, it was observed in one-dimensional systems that, for low polarization, the unpolarized fully paired populations are located at the edges of the cloud while the core is partially polarized [8]. The role of dimensionality in this qualitatively different behavior has been one of the focus of studies on this system. Consequently, the behavior of the system in two dimensions is of considerable interest.

We present here results of our DQMC study of the trapped two-dimensional system. The presence of the trap imposes constraints which make the simulations much harder than the uniform case. The number of particles should be large enough so that at large P, the minority population will still be appreciable but not so large that the local density in the core regions is close to half-filling. Another constraint is that the size of the lattice be large enough to ensure that particles do not leak out. These constraints limit our ability to do simulations for system sizes beyond 20×20.

As for the uniform system, the most important indicator of the presence of the FFLO state is the pair momentum distribution. Although the plane-wave basis is not the natural one in the harmonically confined case, we study the momentum distributions because they are of experimental interest. We will show that despite the shortcomings of this language, one can still detect the FFLO pairing signal this way. In addition, since the trap destroys translational invariance, it is very useful to study the density profiles and local magnetization $m(x,y) = \rho_2(x,y) - \rho_1(x,y)$ where ρ_2 (ρ_1) is local density of the majority (minority). We start with the unpolarized system. Figure 15(a) shows the momentum distribution of the particles (the two populations are identical) for a system with a total of 22.3 particles, $P = 0$, $\beta = 10$, $U = -3.5$, and a lattice size of 20×20. The trap potential is given by $V_t = 0.065$. Figure 15(b) shows the pair momentum distribution and exhibits a sharp peak at zero momentum. Now, we polarize the system keeping the total number of particles constant, which corresponds to the experimental situation. Figure 16 shows the momentum distributions of the (a) minority and (b) majority populations and (c) the pairs. The system has a total of 21.4 particles, $P = 0.55$, $\beta = 10$, $U = -3.5$ and a trap potential $V_t = 0.065$ on a 20×20 lattice. The Fermi temperature of the system is $T_F = 1.86$. Figure 16(c) is qualitatively different from Fig. 15(b) and shows clearly that when the confined system is polarized, it exhibits FFLO states with pairs forming with nonzero center-of-mass momentum. This behavior was observed for a wide range of polarizations and interaction strengths. The vertical scale in Fig. 16(c) shows that the number of pairs is very small. This is due to the small total number of particles in the system. A simulation for a larger system but with the same characteristic density [38] should give a stronger signal in the form of higher peaks at nonzero momentum. This effect of the total number of particles was shown in the one-dimensional uniform case in Ref. [9].

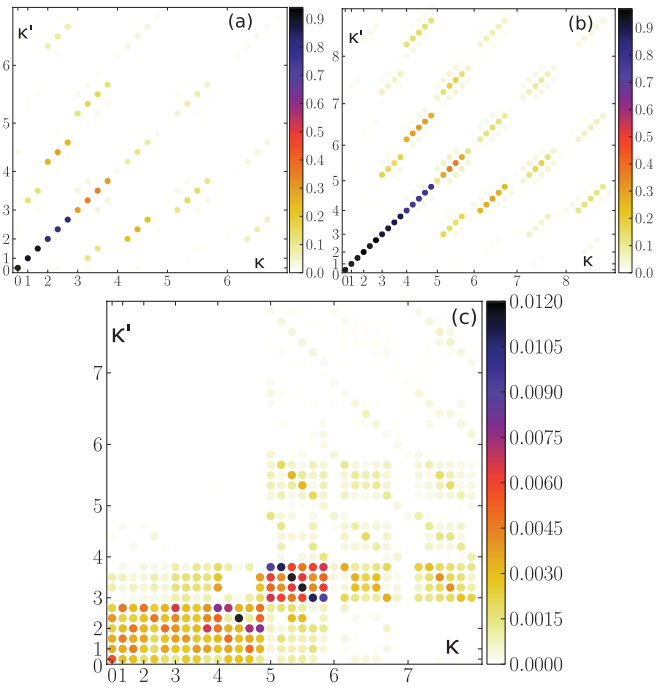

FIG. 13. (Color online) Single particle and pair Green's functions in the harmonic level basis (QMC results) for a strong polarization ($P = 0.37$). The total number of particles is 27.4. The pairing occurs between the levels $n = 5$ and 3 and also $n = 4$ and 2, i.e., with total zero orbital angular momentum. Still, there is small contribution to pairing between $\kappa = (5,-5)$ and $\kappa' = (3,3)$ and $\kappa = (5,5)$ and $\kappa' = (3,-3)$.

During our simulations, we measure the density profiles of each species and we calculate the local magnetization $m(x,y) = n_1(x,y) - n_2(x,y)$. The profiles shown in Fig. 17 correspond to the situation when FFLO-type pairing has been observed in the system as in Fig. 16. One observes that the system is partially polarized at the core and fully polarized in the wings (where we see no minority particles). There is no

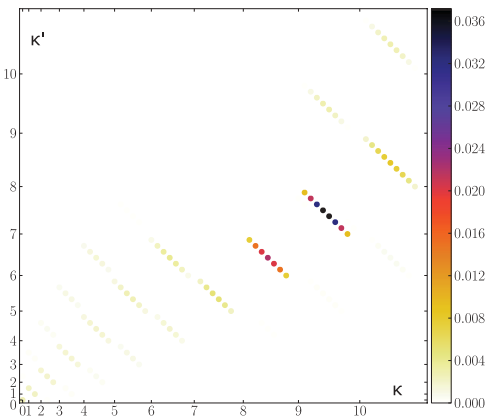

FIG. 14. (Color online) Pair Green's function in the harmonic level basis (MF results) for a polarization $P = 0.27$. The results are similar to the QMC results: pairing is maximum among the Fermi levels $n = 7$ and 9 and also among the two levels below $n = 6$ and 8. The largest m values are almost unpaired, for they would have led to nonzero total angular momentum.

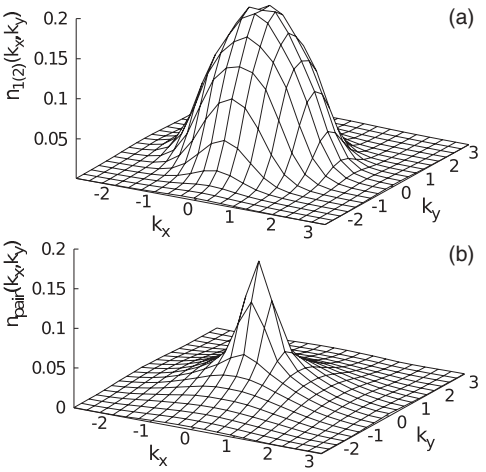

FIG. 15. Momentum distributions of (a) the single particles $n_1(k_x,k_y) = n_2(k_x,k_y)$ and (b) the pairs $n_{\text{pair}}(k_x,k_y)$. The total number of particles is 22.3, $P = 0$, $\beta = 10$, $U = -3.5$, the trap potential is $V_t = 0.065$, and the lattice size 20×20.

fully paired phase where $m(x,y)$ would disappear within the size of the cloud.

Density profiles are the basic quantities that characterize the trapped system. The first experimental results in a three-dimensional system show the formation of concentric shells where for very low polarization the core is fully paired (no local magnetization) and the wings are partially polarized (see [6] and [7]). On the other hand, in the one-dimensional system it has been observed that there exists a low-polarization

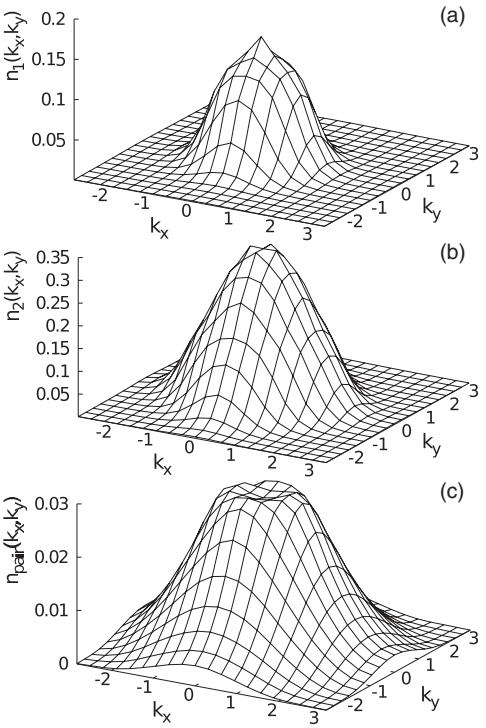

FIG. 16. The momentum distributions of (a) the minority and (b) majority populations and (c) the pairs. The total number of particles is 21.4, $P = 0.55$, $\beta = 10$, $U = -3.5$ on a 20×20 lattice. The trap potential is $V_t = 0.065$ and the Fermi temperature is $T_F = 1.86$.

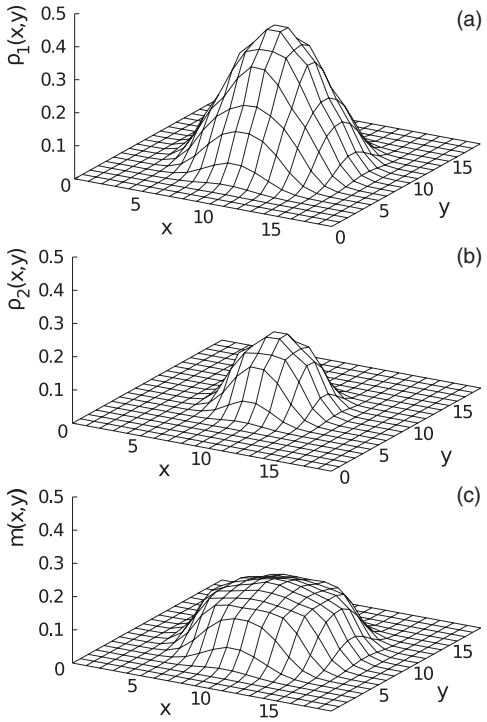

FIG. 17. Density distributions of majority $[n_1(x,y)]$, minority $[n_2(x,y)]$, and the local magnetization $[m(x,y)]$. Total number of particles is 21.4, $P = 0.55$, $\beta = 10$, lattice size 20×20, trap potential $V_t = 0.065$.

regime where the unpolarized superfluid is located at the edge of the cloud, and the core is partially polarized [8]. The issue of this dimensionally driven transition caused considerable interest. It is interesting to look at the intermediate two dimensions and study the behavior of the density profiles to see whether it follows more closely any of the two limiting scenarios. During our simulations, we measure the density profiles of each species and calculate the local magnetization $m(x,y) = n_1(x,y) - n_2(x,y)$. The profiles shown in Fig. 17 correspond to the situation where FFLO-type pairing has been observed in the system as in Fig. 16. One observes that the system is partially polarized at the core and fully polarized in the wings (where we see no minority particles). There is no fully paired phase where $m(x,y)$ would disappear within the size of the cloud.

In the very low-polarization regime, we observe oscillations appearing in the profile of the local magnetization. We looked in detail into these results in order to establish whether the oscillations are linked to the FFLO-type pair density-wave behavior. We found, however, that the oscillations are present in the system even when there is no interaction between particles as seen in Fig. 18. From the discussion in the preceding section, where we have shown the relevance of the harmonic levels at low fillings, we believe that this effect stems from the underlying harmonic level structure. In the balanced case, it has already been shown that the density of a fermionic cloud in a trap can exhibit oscillations with minima or maxima in the center of the trap depending on whether the last filled state corresponds to an odd or even harmonic level [39].

Harmonically confined system around half-filling MF study. As mentioned earlier, the quantum Monte Carlo method suffers

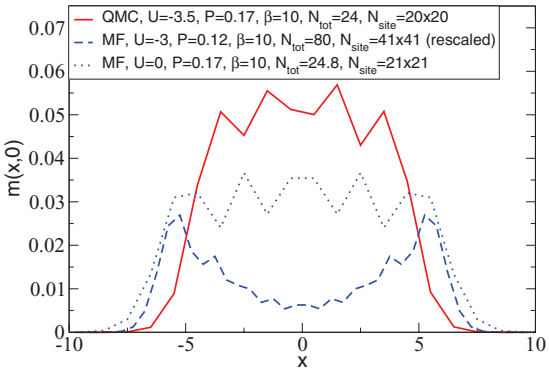

FIG. 18. (Color online) Cut through the center of the trap showing the local magnetization $[m(x,y)]$. Comparison of interacting and noninteracting profiles for low polarization using MF and QMC. The oscillations seen in the magnetization are present even in the noninteracting situation (dashed line). From both the MF and QMC, one can see that the interaction might change the profile, but does not crucially change the oscillation pattern. Therefore, we attribute the oscillations to the underlying harmonic levels rather than to the FFLO order.

from a stronger sign problem for higher fillings of the lattice with the trap. However, we successfully studied the system imbalance around half-filling of the lattice in the trap using the mean-field method. In Figs. 19–22, the order parameter is shown in real space as well as in Fourier space, for increasing value of the polarization. The numerical results were obtained for a lattice size 41×41, an interaction strength $U = -5$, and chemical potential at the center of the trap corresponding to half-filling.

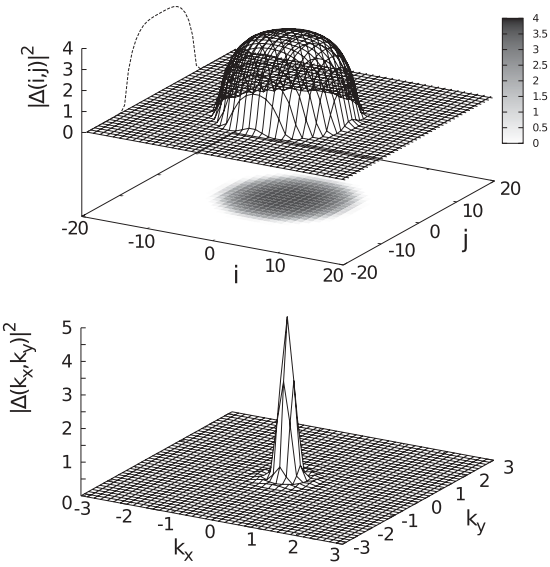

FIG. 19. Mean-field parameter Δ as a function of the position (top) and in Fourier space (bottom) for a low-polarization value ($P = 0.13$), around the half-filling situation, in the presence of an harmonic trap. The structure is similar to the balanced case, i.e., a maximum number of pairs at the center of the trap, decreasing on the border. The Fourier transform simply depicts a peak at $\vec{k} = 0$, emphasizing a BCS-type pairing.

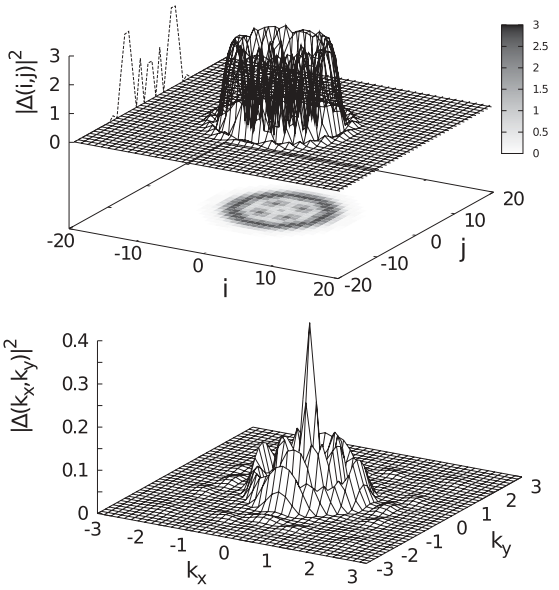

FIG. 20. Mean-field parameter Δ as a function of the position (top) and in Fourier space (bottom) for a polarization value $P = 0.43$. A structure in the center of the trap is clearly visible, leading to oscillations in the Fourier transform.

At low polarization ($P = 0.13$) (Fig. 19), the structure is similar to the balanced case, i.e., a maximum number of pairs at the center of the trap, decreasing on the border. The Fourier transform simply depicts a peak at $\vec{k} = 0$, emphasizing BCS-type pairing. At higher polarization $P = 0.43$ (Fig. 20), a structure in the pairing order Δ appears at the center of the trap, leading to clear oscillations in Fourier space. This pattern appears first at the center of the trap simply

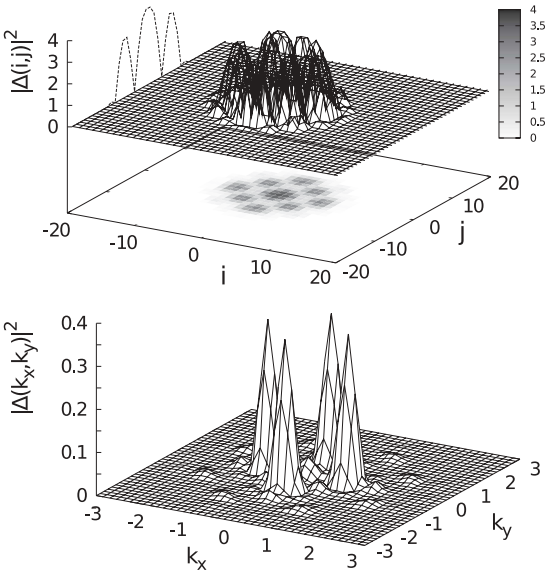

FIG. 21. Mean-field parameter Δ as a function of the position (top) and in Fourier space (bottom) for a polarization value $P = 0.48$. The checkerboard pattern is a clear signature of the FFLO state. The Fourier transform depicts four peaks at the positions $(kx = 0, ky = \pm q)$ and $(kx = \pm q, ky = 0)$, precisely like in the homogeneous situation at half-filling.

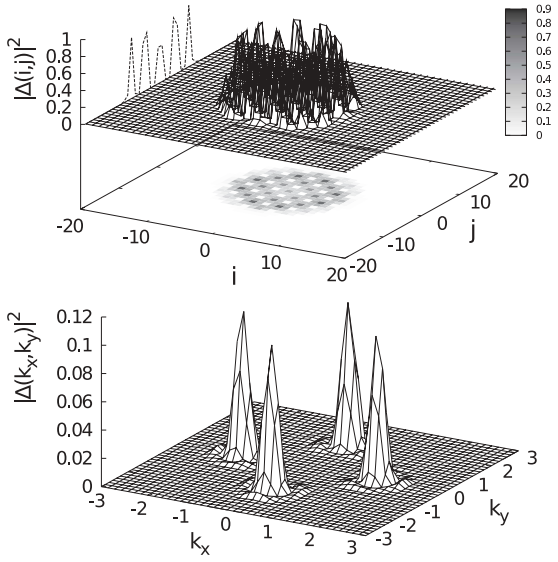

FIG. 22. Mean-field parameter Δ as a function of the position (top) and in Fourier space (bottom) for a polarization value $P = 0.66$. The checkerboard pattern depicts now a shorter period in real space, translating into a larger spreading of the four peaks in the Fourier space and corresponding to pairs having a larger center-of-mass momentum compared to Fig. 21.

because it corresponds to half-filling which, as explained in a previous section, is strongly unstable towards the FFLO state. Indeed, this is emphasized by Figs. 21 and 22 corresponding, respectively, to polarization $P = 0.48$ and 0.66. The checkerboard pattern of $|\Delta|^2$ in real space becomes more and more visible. Note that similar results have been previously shown in Ref. [40]. However, we would like to emphasize the link between this pattern and the nature of the pairing in the homogenous situation. Indeed, in Fourier space, four peaks are clearly observed. Their positions $(k_x = 0, k_y = \pm q)$ and $(k_x = \pm q, k_y = 0)$ precisely match those observed in the homogeneous situation, both in the QMC results and in the MF ones, around half-filling. In addition, one can see that the oscillation period of the order parameter becomes shorter with higher polarization, i.e., corresponding to a larger center-of-mass momentum q of the pair, which is depicted by the spreading of the four peaks further away from $\vec{k} = 0$. This also shows that the oscillations in real space are not related to the underlying harmonic levels, but really to the FFLO order. From the experimental point of view, this signature of the FFLO order could be measured either directly in the density of pairs or in their velocity distribution. Of course, the present mean-field calculation does not include the thermal fluctuations which are crucial to properly describe the condensation of the pairs which, at large interaction, arises at a temperature $k_B T \approx t^2/U$ lower than the pair formation temperature $k_B T \approx U$ [34,41–43].

V. CONCLUSIONS

Our results, based on QMC and MF calculations, strongly emphasize that the FFLO state is the ground state of the fermionic Hubbard model on the square lattice for a large range of parameters, both with or without harmonic confinement. At

low filling, the FFLO state is similar to the bulk situation (i.e., particles having a quadratic dispersion relation), where the pairs have a vanishing total angular momentum, but a finite radial component for the center-of-mass momentum. On the contrary, around half-filling, the underlying Fermi surface due to the lattice structure leads to a FFLO state having only discrete value of the center-of-mass momentum, namely, around $(kx = 0, ky = \pm q)$ and $(kx = \pm q, ky = 0)$. We have given an explanation in terms of matching fermionic momentum on the Fermi surfaces. We have also shown that, in the presence of a harmonic confinement and at low fillings, the harmonic level basis gives rise to a simple understanding of the pairing mechanism. In addition, we have shown that the harmonic levels are at the origin of the oscillations seen in the local magnetization, which, therefore, are not a signature of the FFLO state. Finally, still in the presence of a harmonic confinement, but around half-filling, we have shown that the pairing mechanism is essentially identical to the homogeneous situation, leading to clear signatures in the pair density, both in real space (checkerboard pattern) and in Fourier space (four peaks), which allows for a possible experimental observation with cold atoms.

In the presence of a harmonic trap, it would be interesting to study the dynamics of the pairs in response to a sudden quench from balanced to imbalanced populations where our study indicates that one could expect to observe the oscillations of the center of mass in the trap. In addition, from a mean-field point of view, the following points would be interesting to consider. By monitoring the wavelength and the amplitude of the oscillations of the order parameter, one should be able to determine the nature of the pairing and possible transitions between paired phases. One should also take into account the effects of terms beyond mean field to determine properly the critical temperature of the transition (BKT-type) and to estimate the strength of the quantum fluctuations, thus allowing for a better comparison with possible experimental results. Finally, one could study more exotic situations, such as asymmetric tunneling rates, or in the presence of an effective gauge field.

ACKNOWLEDGMENTS

We thank C. Miniatura for very helpful discussions. This work was supported by an ARO Award No. W911NF0710576 with funds from the DARPA OLE Program; by the CNRS-UC Davis EPOCAL joint research grant; by the France-Singapore Merlion program (PHC Egide and FermiCold 2.01.09), and by the LIA FSQL. Centre for Quantum Technologies is a Research Centre of Excellence funded by the Ministry of Education and National Research Foundation of Singapore.

[1] J. Bardeen, L. N. Cooper, and J. R. Schrieffer, Phys. Rev. **108**, 1175 (1957).
[2] P. Fulde and A. Ferrell, Phys. Rev. **135**, A550 (1964).
[3] A. Larkin and Y. N. Ovchinnikov, Zh. Eksp. Teor. Fiz. **47**, 1136 (1964) [Sov. Phys.–JETP **20**, 762 (1965)].
[4] G. Sarma, Phys. Chem. Solids **24**, 1029 (1963); S. Takada and T. Izuyama, Prog. Theor. Phys. **41**, 635 (1969).
[5] H. A. Radovan, N. A. Fortune, T. P. Murphy, S. T. Hannahs, E. C. Palm, S. W. Tozer, and D. Hall, Nature (London) **425**, 51 (2003).
[6] M. W. Zwierlein, A. Schirotzek, C. H. Schunck, and W. Ketterle, Science **311**, 492 (2006); M. W. Zwierlein, C. H. Schunck, A. Schirotzek, and W. Ketterle, Nature (London) **422**, 54 (2006); Y. Shin, M. W. Zwierlein, C. H. Schunck, A. Schirotzek, and W. Ketterle, Phys. Rev. Lett. **97**, 030401 (2006); Y. Shin, C. H. Schunck, A. Schirotzek, and W. Ketterle, Nature (London) **451**, 689 (2008).
[7] G. B. Partridge, W. Li, R. I. Kamar, Y. Liao, and R. G. Hulet, Science **311**, 503 (2006); G. B. Partridge, W. Li, Y. A. Liao, R. G. Hulet, M. Haque, and H. T. C. Stoof, Phys. Rev. Lett. **97**, 190407 (2006).
[8] Y. Liao, A. S. C. Rittner, T. Paprotta, W. Li, G. B. Partridge, R. G. Hulet, S. K. Baur, and E. J. Mueller, Nature (London) **467**, 567 (2010).
[9] G. G. Batrouni, M. H. Huntley, V. G. Rousseau, and R. T. Scalettar, Phys. Rev. Lett. **100**, 116405 (2008).
[10] M. Casula, D. M. Ceperley, and E. J. Mueller, Phys. Rev. A **78**, 033607 (2008).
[11] A. E. Feiguin and F. Heidrich-Meisner, Phys. Rev. B **76**, 220508(R) (2007).
[12] A. Lüscher, R. M. Noack, and A. M. Läuchli, Phys. Rev. A **78**, 013637 (2008).
[13] M. Rizzi, M. Polini, M. A. Cazalilla, M. R. Bakhtiari, M. P. Tosi, and R. Fazio, Phys. Rev. B **77**, 245105 (2008).
[14] M. Tezuka and M. Ueda, Phys. Rev. Lett. **100**, 110403 (2008).
[15] F. Heidrich-Meisner, A. E. Feiguin, U. Schollwöck, and W. Zwerger, Phys. Rev. A **81**, 023629 (2010).
[16] M. M. Parish, S. K. Baur, E. J. Mueller, and D. A. Huse, Phys. Rev. Lett. **99**, 250403 (2007).
[17] D.-H. Kim, J. J. Kinnunen, J.-P. Martikainen, and P. Törmä, Phys. Rev. Lett. **106**, 095301 (2011).
[18] M. J. Wolak, V. G. Rousseau, C. Miniatura, B. Grémaud, R. T. Scalettar, and G. G. Batrouni, Phys. Rev. A **82**, 013614 (2010).
[19] T. K. Koponen, T. Paananen, J.-P. Martikainen, M. R. Bakhtiari, and P. Törmä, New J. Phys. **10**, 045014 (2008).
[20] Y. L. Loh and N. Trivedi, Phys. Rev. Lett. **104**, 165302 (2010).
[21] D. E. Sheehy and L. Radzihovsky, Ann. Phys. (NY) **322**, 1790 (2007).
[22] M. M. Parish, F. M. Marchetti, A. Lamacraft, and B. D. Simons, Nat. Phys. **3**, 124 (2007).
[23] A. Bulgac and Michael McNeil Forbes, Phys. Rev. Lett. **101**, 215301 (2008).
[24] K. Machida, T. Mizushima, and M. Ichioka, Phys. Rev. Lett. **97**, 120407 (2006).
[25] L. He and P. Zhuang, Phys. Rev. A **78**, 033613 (2008).
[26] B. Van Schaeybroeck, A. Lazarides, S. Klimin, and J. Tempere, arXiv:0911.0984.
[27] S. M. A. Rombouts, arXiv:0902.1450.
[28] Theja N. De Silva, J. Phys. B: At. Mol. Opt. Phys. **42**, 165301 (2009).
[29] Z. Cai, Y. Wang, and C. Wu, Phys. Rev. A **83**, 063621 (2011).
[30] A. E. Feiguin and F. Heidrich-Meisner, Phys. Rev. Lett. **102**, 076403 (2009).

[31] R. Blankenbecler, D. J. Scalapino, and R. L. Sugar, Phys. Rev. D **24**, 2278 (1981); S. R. White, D. J. Scalapino, R. L. Sugar, E. Y. Loh, J. E. Gubernatis, and R. T. Scalettar, Phys. Rev. B **40**, 506 (1989).
[32] M. Iskin and C. J. Williams, Phys. Rev. A **78**, 011603(R) (2008).
[33] Y. Fujihara, A. Koga, and N. Kawakami, Phys. Rev. A **81**, 063627 (2010).
[34] B. Grémaud, Europhys. Lett. **98**, 47003 (2012).
[35] T. Paiva, R. R. dos Santos, R. T. Scalettar, and P. J. H. Denteneer, Phys. Rev. B **69**, 184501 (2004).
[36] J. Tempere, S. N. Klimin, and J. T. Devreese, Phys. Rev. A **79**, 053637 (2009).
[37] B.-G. Englert, *Lectures on Quantum Mechanics* (World Scientific, Singapore, 2006), Vol. 2, p. 129.
[38] M. Rigol, G. G. Batrouni, V. G. Rousseau, and R. T. Scalettar, Phys. Rev. A **79**, 053605 (2009).
[39] G. M. Bruun and K. Burnett, Phys. Rev. A **58**, 2427 (1998).
[40] Y. Chen, Z. D. Wang, F. C. Zhang, and C. S. Ting, Phys. Rev. B **79**, 054512 (2009).
[41] J. R. Engelbrecht, M. Randeria, and C. A. R. Sá de Melo, Phys. Rev. B **55**, 15153 (1997).
[42] M. Iskin and C. A. R. Sá de Melo, Phys. Rev. A **76**, 013601 (2007).
[43] J. Tempere, S. N. Klimin, and J. T. Devreese, Phys. Rev. A **78**, 023626 (2008).